Nat. Volatiles & Essent. Oils, 2021;8(4):16908-16919

Characterization And Compatibility Studies Of Valsartan With Pharmaceutical Excipients

Dr. K. Atchuta Kumar[1]*

[1]*Professor, Bhaskara Institute of Pharmacy, Komatipalli, Bobbili, Andhra pradesh

***Corresponding Author:** Dr. K. Atchuta Kumar
E-mail: dratchut99@gmail.com

Abstract:
The thermal analytical study of valsartan chemically *N*-(1-oxopentyl) - *N*-[[2'-(1H-tetrazol-5-yl) [1, 1'-biphenyl] - 4-yl] methyl]-L-valine, an anti-hypertensive was investigated using differential scanning calorimetry (DSC), X-ray powder diffraction (XRPD), Fourier transform infrared spectroscopy (FTIR), scanning electron microscopy (SEM). The DSC curves have shown a sharp endothermic event at 101.16°C. Solid state characterization was carried out by FTIR, scanning electron microscopy SEM, and XRPD demonstrating the drug physicochemical properties including crystallinity. Drug-excipient compatibility studies investigated by DSC with different excipients like Magnesium stearate, Sodium starch glycolate, Potato starch, Crospovidone, Croscarmellose, Sodium Starch Glycolate, PolyEthyleneGlycol 6000, pregelatizedstarch, talc, lactose, polyvinylpyrollidine K30, sodiumcarboxymethyl cellulose, micro crystalline cellulose. DSC spectra's has shown a possible physical interaction of the drug with magnesium stearate, polyvinylpyrollidine K30 (PVP K30), PolyEthyleneGlycol 6000 (PEG 6000) and Potato starch.

1. INTRODUCTION

Hypertension is one of the most prevalent chronic adult illnesses today and cannot be cured, but it can be controlled[1]. The pharmacological treatment for control of hypertension utilizes various drug therapies, single doses or associations of diuretics, beta-blockers, calcium channel blockers, angiotensin converting enzyme (ACE) inhibitors and angiotensin II receptor (AT1) antagonist (ARA)[2–5]. Valsartan (VAL, Figure 1) is one of the angiotensin II receptor (AT1) antagonists recommended for treatment of hypertension, post-myocardial infarction or congestive heart failure and chemically it is N-(1-oxopentyl)-N-[[2'-(1H-tetrazol-5-yl)[1,1'-biphenyl]-4-yl]methyl]-L-valine1.

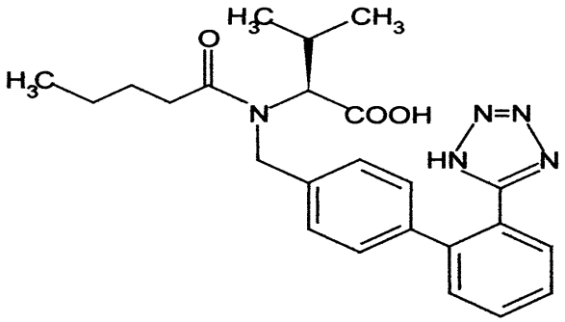

Fig.1. Chemical structure of Valsartan.

Thermal analyses are routine methods for analysis of drugs and substances of pharmaceutical interest. These methods include differential scanning calorimetry (DSC) and thermogravimetry (TG), in which physical properties of a substance and/or its reaction products are measured as function of a controlled temperature

program. Studying the drug-excipient compatibility during the formulation of products is an important process to know any physical and chemical interaction between the compounds. Thermal techniques have been increasingly used for evaluating possible incompatibility quickly through comparison of thermal curves of pure substances with curve obtained from a 1:1 mixture[6].
The characterization of solid-state properties at an early stage by using appropriate analytical methodologies is an essential pre-requisite in the development of solid dosage forms both from scientific and regulatory points of view. Variations in physicochemical properties of the pharmaceutical active ingredient may have an impact on the therapeutic, manufacturing, commercial, and legal levels[7–10].
In this work, the Valsartan characterization and compatibility studies have been investigated by using a variety of techniques including thermal analysis (TG/DTG and DSC), Fourier transform infrared spectroscopy (FTIR), scanning electron microscopy (SEM), and X-ray powder diffraction (XRPD)[11, 12].

2. Experimental

2.1 Materials

Valsartan bulk material was obtained from Aurobindo Pharma. Hyderabad. The tested pharmaceutical excipients in the compatibility studies were: magnesium stearate; potato starch; crospovidone; croscarmellose; sodium starch glycolate (SSG);polyethyleneglycol (PEG) 6000 ; pregelatizedstarch (PG starch); talc; lactose; polyvinylpyrrolidone (PVP) K30; sodiumcarboxymethyl cellulose (Na CMC) and microcrystallinecellulose (MCC).

2.2 Preparation of physical mixtures

The interaction study was performed by using a physical mixture of Valsartan and excipients of equal weights (1:1 mass/mass). Each material (drug & excipient) is sieved and the respective 75-150 µm fractions used. Physical mixtures (300 mg) were prepared by blending equal amounts of drug and each excipient in a glass bottle and analysed.

2.3 Methods

2.3.1 Differential scanning calorimetry (DSC)

The DSC curves were obtained using a Mettler Toledo DSC apparatus under dynamic nitrogen atmosphere with the flow rate of 50 mL min-1. Approximately 2-5 mg of samples were weighted out and placed in a sealed aluminum pan. The analysis was carried out from 30 to 200°C at a heating rate of 10°C min^{-1}.

2.3.2 Fourier transform infrared spectroscopy (FTIR)

Fourier transform infrared (FTIR) spectra (in cm–1) were recorded from 4000 to 400 cm–1 with a resolution of 4 cm–1 using the PerkinElmer Spectrum BX spectrometer. The spectra were scanned by averaging 16 scans for each transmission spectrum. Before performing the FTIR spectrum of the substance in the KBr pellet, a background spectrum with the atmosphere as reference was recorded. Thus the spectral features of the air ingredient do not interfere with spectra of the substance. Samples for IR studies were prepared by mixing 1mg of the analyzed substance with about 99 mg of spectral grade KBr and compressing in a hand-held minipress at 60 tons for 1min[12].

2.3.3 X-ray powder diffraction (XRPD)

X-ray diffraction patterns of the samples were recorded, using X-ray diffractometer, Brucker AXSD8 Advance with Cu-Kα (Ni-filter), radiation (λ= 1.5418 °A). The experiments were carried out at room temperature under the following conditions: voltage 20 kV, current 20 mA, 2θ angle range 10-60 with scanning speed, 5°/minute[13].

2.3.4 Scanning electron microscopy (SEM)

The surface morphology of the raw materials and of the binary systems was examined by means of Hitachi SEM (Tokyo Japan). The powders were precisely fixed on an aluminium stub using double-sided adhesive

tape and then were made electrically conductive by coating in a vaccum with a thin layer of gold for 30 seconds and at 30 W[14].

3. Results and discussion

3.1 Characterization of Valsartan

The DSC and TGA curves obtained for Valsartan are shown in Fig.2, 3. The untreated pure drug was sieved and the respective 75- 150 µm fraction used. The DSC curve has shown a sharp endothermic event (Tpeak = 101.16°C; Tonset = 96.47 °C) corresponding to the melting point followed by decomposition. The TG/DTG curve has shown a single stage of mass loss between 254–283 °C and degradation of drug shows temperature at 292.28°C. The DSC data combined with TG allow evidencing a thermal stability up to 200 °C.

SEM photomicrographs that reveal the surface morphology of the samples. SEM photomicrograph of Valsartan was shown in Fig.4. The Characteristic needle-shaped poor crystals of Valsartan were observed in the photomicrograph. It provides additional information than the XRPD. The drug shows with small particle size of about 10µm diameter. [15–18]

A XRPD spectrum of Valsartan was shown in Fig.5. XRPD spectrum reveals that pure drug Valsartan shows poor crystalline nature. The diffraction pattern of the pure drug Valsartan shows poor crystalline nature, indicated by less distinctive peaks at a diffraction angle of 2θ (5.2°, 14.6°, 18.8°, 17°) throughout the scanning range.

The FTIR spectrum of untreated Valsartan is shown in Fig.6. The Valsartan at room temperature showed absorption band assigned to NH-C=O group at 1,602 cm-1 that is characteristic of the amide and C=O group at 1730.45 cm-1 that is characteristic of the carbonate group. The absorption bands at 1160, 1105 and 1051 cm-1 assigned to asymmetric stretching of C–O in carbonate group and symmetric stretching of C–O in amide group can observed respectively. The absorption bands at 759 cm-1 assigned to asymmetric stretching of N–H in amine group. Furthermore, the broad absorption band at 3447 cm-1assigned to stretching of O–H and the absorption band at 2962 cm-1 assigned to stretching of N–H[19].

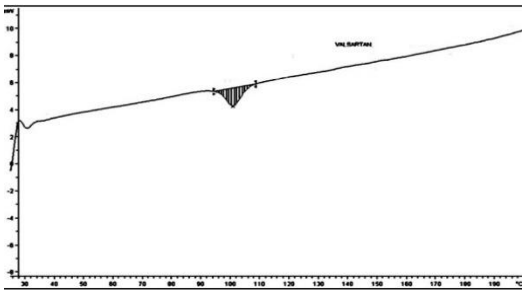

Fig.2 DSC curve of Valsartan obtained in dynamic nitrogen atmosphere (50 mL min-1) and heating rate of 10 °C min-1

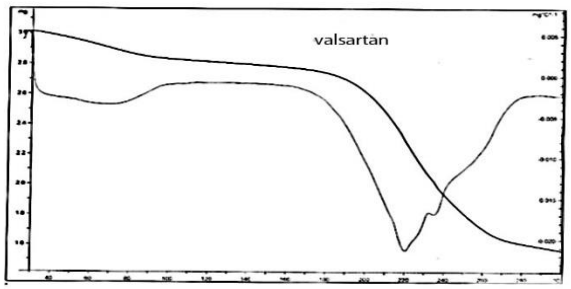

Fig.3 TGA curve of Valsartan obtained in dynamic nitrogen atmosphere (50 mL min-1) and heating rate of 10 °C min-1

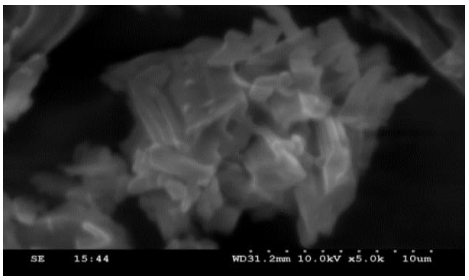

Fig.4. SEM photomicrograph of Valsartan

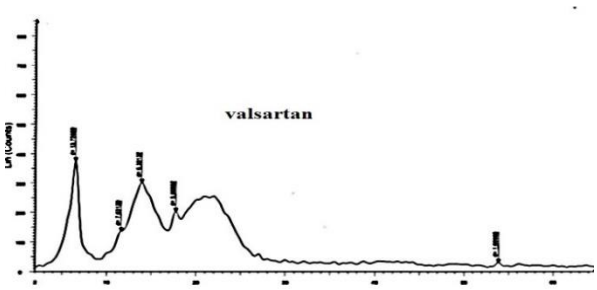

Fig.5. X-ray powder diffraction of Valsartan

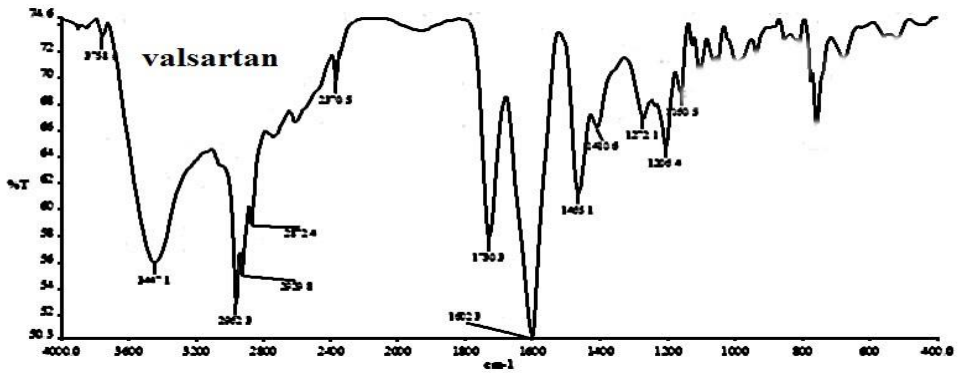

Fig. 6 FTIR spectrum of Valsartan

3.2 Compatibility studies with excipients

3.2.1 Differential Scanning Calorimetry (DSC)

In fact, DSC has been proposed to be a rapid method for evaluating physicochemical interactions between components of the formulation through the comparison of thermal curves of pure substances with the curve obtained from a 1:1 physical mixture and therefore select adequate excipients with suitable compatibility[20–22].

The thermal profiles of the mixtures Valsartan/talc, Valsartan/SSG, Valsartan/lactose, Valsartan/ Crospovidone, Valsartan/Croscarmellose, Valsartan/Na CMC, Valsartan/MCC, Valsartan/PG starch can be considered as a superposition of the curves of Valsartan and excipients, demonstrating the absence of interaction.

The DSC curve of Valsartan/talc has shown the characteristic endothermic event of Valsartan melting point at 101.16°C as shown in Fig.7. It shows no incompatibility between drug and talc mixture (1:1). In Valsartan/ lactose has shown the characteristic endothermic event of Valsartan melting point at 100.99°C as shown in Fig.8. Valsartan/Crospovidone has shown an endothermic event at 100.42°C as shown in Fig.9 which is the characteristic endothermic melting point of Valsartan. In Valsartan/Croscarmellose as shown in Fig.10 the curves shows broad endothermic event between 25-80°C due to the dehydration of Croscarmellose followed

by the characteristic endothermic event of Valsartan melting point at 100.87°C. Valsartan/Na CMC has shown an endothermic event between 70 to 85°C due to dehydration of excipient Na CMC followed by Valsartan melting point peak at 100.49°C as shown in Fig 11. In Valsartan/SSG has shown the slight endothermic event between 40-80°C due to the dehydration of SSG followed by characteristic endothermic event of Valsartan melting point at 100.25°C as shown in Fig 12. In Valsartan/MCC has shown the characteristic endothermic event of Valsartan melting point at 100.44°C as shown in Fig.13. In Valsartan/PG starch has shown the broad endothermic event between 25-85°C due to the dehydration of PG starch followed by characteristic endothermic event of Valsartan melting point at 98.21°C as shown in Fig 14[23].

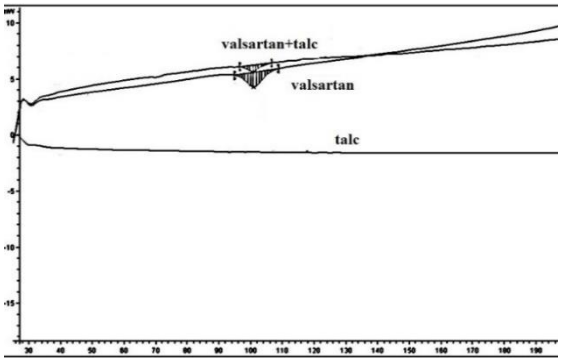

Fig. 7 DSC curves of Valsartan, Talc and mixture of Valsartan and Talc (1:1) .

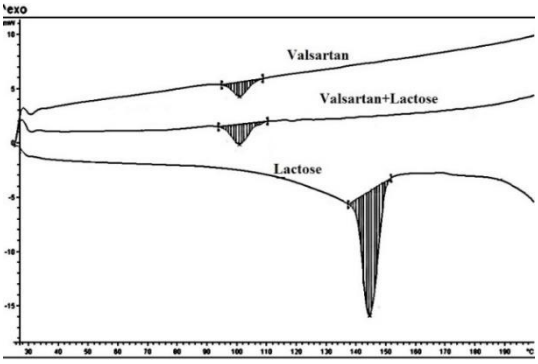

Fig. 8 DSC curves of Valsartan, Lactose and mixture of Valsartan and Lactose (1:1)

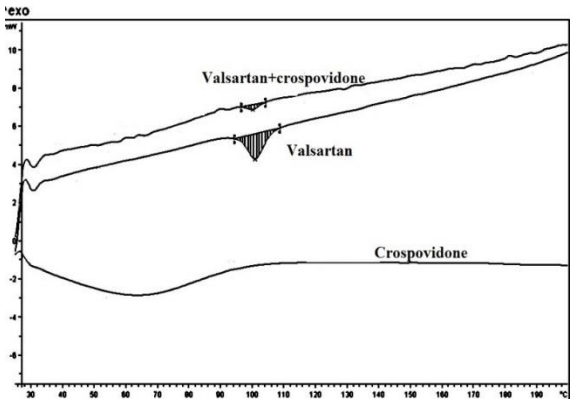

Fig. 9 DSC curves of Valsartan, Crospovidone and mixture of Valsartan and Crospovidone (1:1)

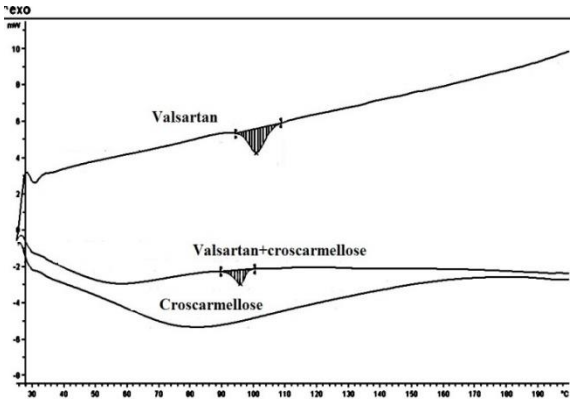

Fig.10 DSC curves of Valsartan, Croscarmellose and mixture of Valsartan and Croscarmellose (1:1)

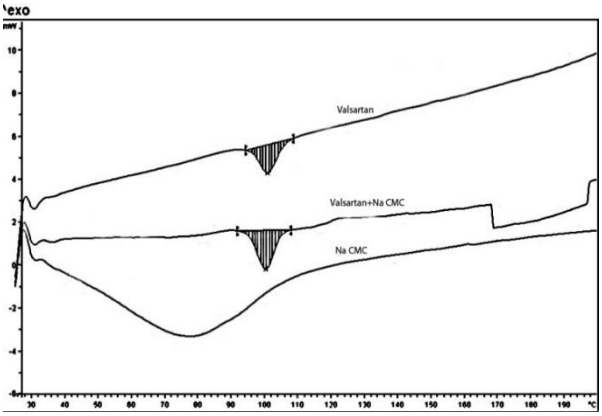

Fig.11 DSC curves of Valsartan, Na CMC and mixture of Valsartan and Na CMC (1:1)

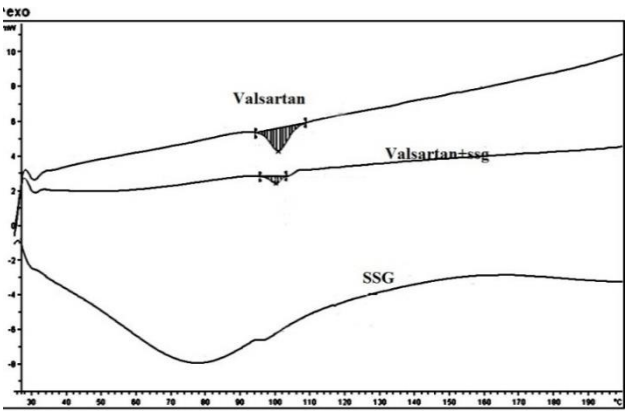

Fig.12 DSC curves of Valsartan, SSG and mixture of Valsartan and SSG (1:1)

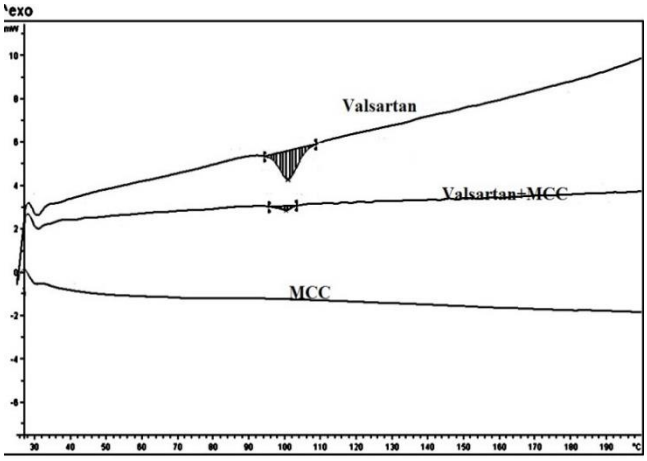

Fig.13 DSC curves of Valsartan, MCC and mixture of Valsartan and MCC (1:1)

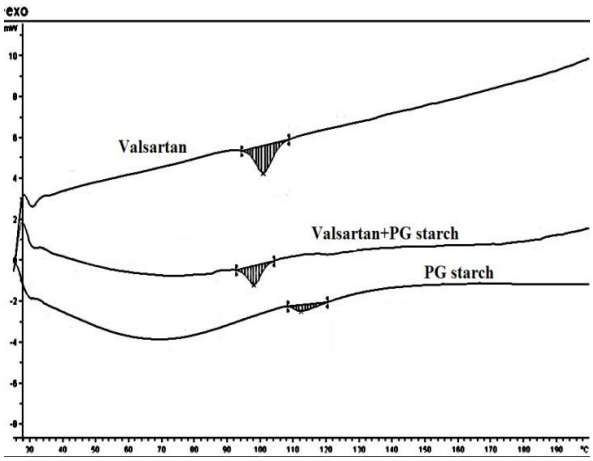

Fig.14 DSC curves of Valsartan, Pregelatinized starch (PG starch) and mixture of Valsartan and PG starch (1:1)

Differences were observed in the DSC curves of Valsartan/ Magnesium stearate, Valsartan/ PVP K30, Valsartan/ PEG 6000 and Valsartan/ potato starch in which the melting point of the drug shifted to a lower temperature of Tpeak = 84.32, 96.47, 64.09 and 95.53°C respectively. These results indicated the occurrence of a strong interaction in the solid state with these excipients corresponding to incompatibility. The results of Valsartan/Magnesium stearate (Fig.15) have shown one endothermic event at 84.32°C due to the presence of impurities like stearic acid and palmitic acid in magnesium stearate, they interact strongly with the drug in high concentrations. Polyvinyl pyrrolidone (PVP) is a synthetic colloid, water soluble and diverse organic solvent, having a high viscosity and the capacity to form complex. DSC curve of Valsartan/PVP k30 (Fig. 16) has shown an endothermic events at 96.47°C, It shows a broad endothermic peak from 25 to 53°C and 60 to 90°C followed by drug melting point peak at 96.47°C. The shift of peak to lower temperatures from 101.16 to 96.47°C due to the presence of more hygroscopic nature of PVP K30 results in dehydration at lower temperatures indicates incompatible with the Valsartan. DSC curve of Valsartan/PEG 6000 (Fig 17) has shown an endothermic event at 64.09°C.PEG 6000 forms clumpy wet mass with the drug and in DSC curve it shows absence of drug melting point at 101.16°C. It shows excipient have strongly interacted with the drug Valsartan and shows incompatibility. DSC curve of Valsartan/Potato starch (Fig 18) has shown an endothermic event at 95.53°C. It shows the shift of drug melting point peak from 101.16°C to 95.53°C due to the larger dehydration of the excipient from 25-160°C. It shows the excipient is incompatible with the drug Valsatan.

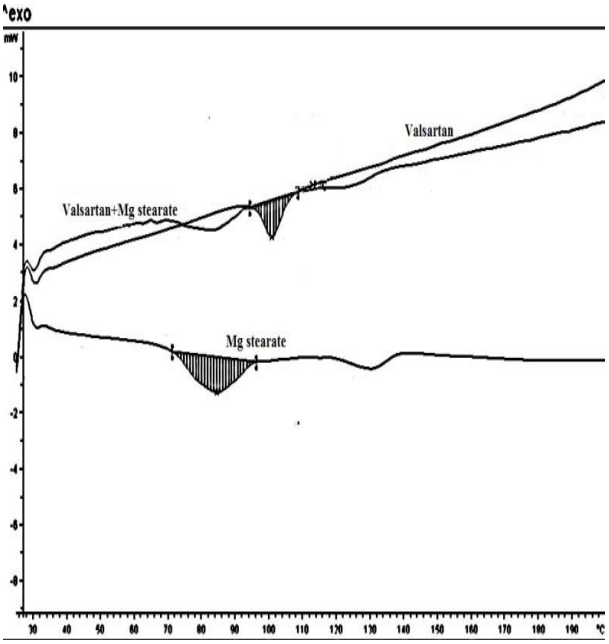

Fig.15 DSC curves of Valsartan, Magnesium stearate and mixture of Valsartan and magnesium stearate

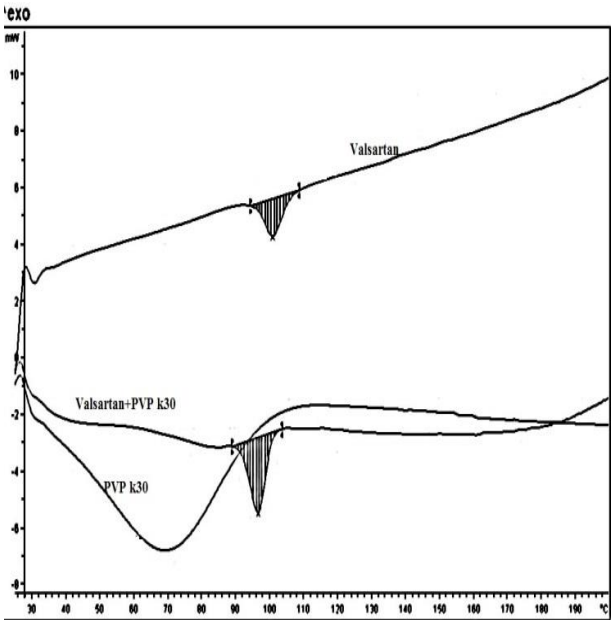

Fig.16 DSC curves of Valsartan, PVP K30 and mixture of Valsartan and PVP K30 (1:1)

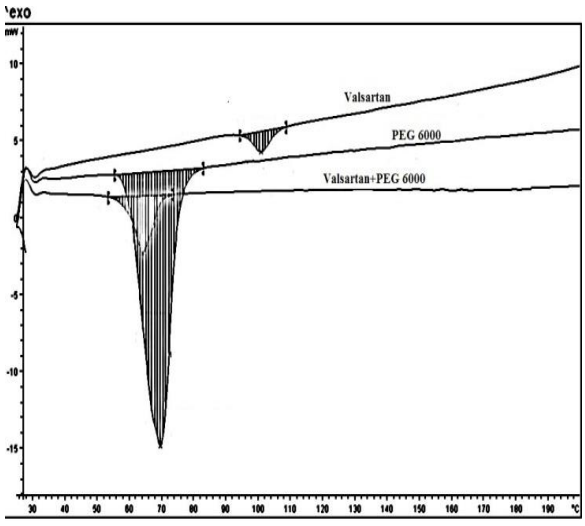

Fig.17 DSC curves of Valsartan, PEG 6000 and mixture of Valsartan and PEG 6000 (1:1)

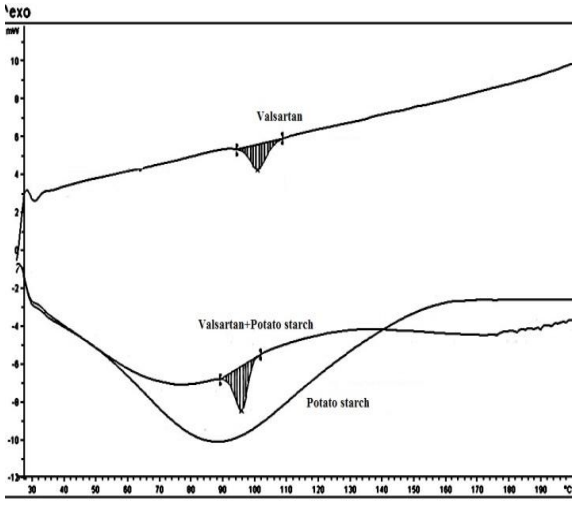

Fig.18 DSC curves of Valsartan, Potato starch and mixture of Valsartan and potato starch (1:1)

Table 1 Thermoanalytical data of Valsartan and drug:excipient physical mixtures

S.No.	Samples	T onset (°C)	T peak(°C)
1.	**Drug (Valsartan)**	96.40	101.16
2.	MCC : Valsartan(1:1)	96.90	100.44
3.	Na CMC:Valsartan(1:1)	95.34	100.49
4.	Magnesium sterate:Valsartan(1:1)	71.64	84.32
5.	Talc :Valsartan(1:1)	97.31	100.87
6.	Lactose:Valsartan(1:1)	95.63	100.99
7.	Crospovidone:Valsartan(1:1)	96.71	100.42
8.	Croscarmellose:Valsartan(1:1)	91.88	95.73
9.	SSG:Valsartan(1:1)	97.02	100.25
10.	PG starch:Valsartan(1:1)	93.94	98.12
11.	Potato starch:Valsartan(1:1)	91.12	95.53
12.	PVP:Valsartan(1:1)	91.52	96.47
13.	PEG 6000:Valsartan(1:1)	59.39	64.09

3.2.2 Fourier transforms infrared spectroscopy

FTIR has been applied as a supplementary technique to investigate drug-excipient interaction and to confirm the results obtained from the thermal analysis. It is the most suitable technique of the non-destructive spectroscopic methods and has become an attractive method in the analysis of pharmaceutical solids, since the materials are not subject to thermal or mechanical energy during sample preparation, therefore preventing solid-state transformations. The appearance of new absorption band(s), broadening of band(s) and alteration in intensity is the main characteristics to evidence interactions between drug and excipients. The spectra of the drug and all excipients used in this study were obtained for pure compounds as well for binary mixtures (1:1 mass/mass) in order to identify a possible chemical interaction between them. The FTIR spectra did not show evidence on chemical interaction in the solid state. Moreover, the spectra of binaries mixtures can be considered as the superposition of the individual ones without absence, shift or broadening in the vibration bands of Valsartan. FTIR spectra's of mixtures of Magnesium stearate and Valsartan (Fig. 19) shows merging of two peaks 1730, 1602 cm–1 to 1541 cm–1. It shows chemically incompatibility between Valsartan and magnesium stearate. An FTIR spectrum of Valsartan and PVP K30 (Fig. 20) also shows merging of two peaks from 1730, 1602 to 1656 cm–1.This indicates PVP K30 shows chemically incompatibility with the drug Valsartan. But FTIR spectra's (Fig 21, 22) demonstrated the absence of chemical interactions between Valsartan, PEG 6000 and potato starch suggesting that the modification showed by DSC curves can be related to a possible physical interaction.

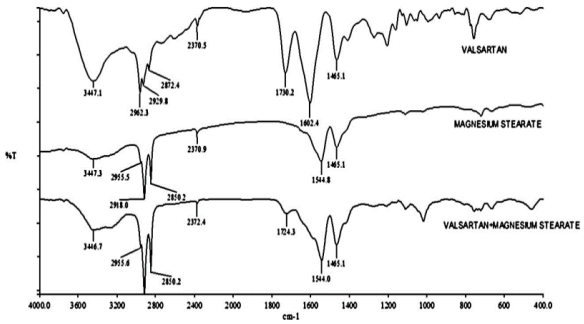

Fig.19. FTIR curves of Valsartan, Magnesium stearate and mixture of Valsartan and Magnesium stearate (1:1)

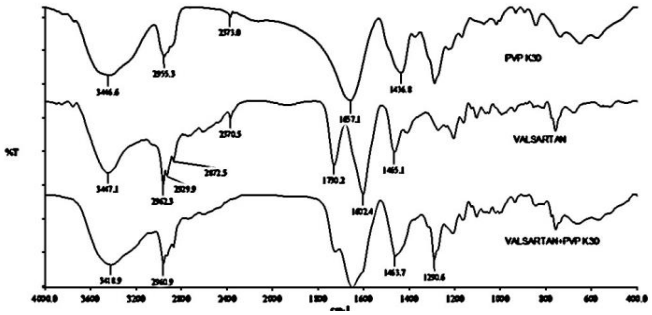

Fig.20. FTIR curves of Valsartan, PVP K30 and mixture of Valsartan and PVP K30 (1:1)

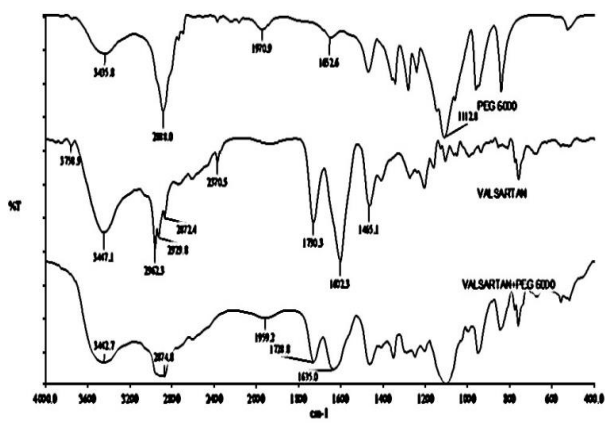

Fig.21. FTIR curves of Valsartan, PEG 6000 and mixture of Valsartan and PEG 6000 (1:1)

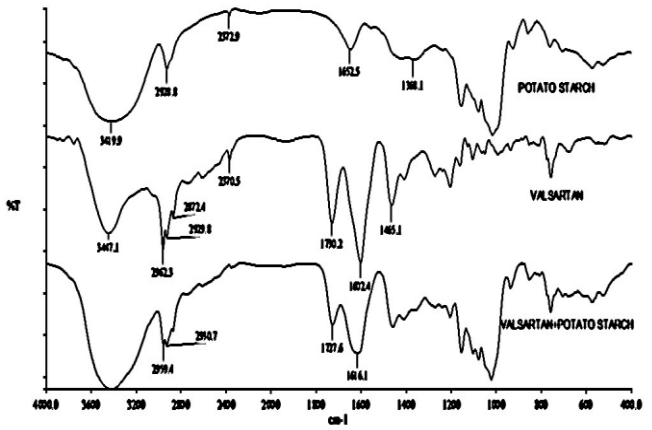

Fig.22. FTIR curves of Valsartan, Potato starch and mixture of Valsartan and Potato starch (1:1)

3.2.3 X-ray powder diffraction

X-ray powder diffraction studies were then performed, in order to obtain more information and to support DSC and FTIR results. The studied drug Valsartan has poor crystalline characteristics. The 2θ values of the less intensive peaks for Valsartan are 2θ = 5.2°, 14.6°, 17°, 18.8°. In Fig. 23 the X-ray powder diffractograms of Valsartan and the binaries can be observed.

According to our experiences, XRPD evidence shows incompatibility only between Valsartan and the magnesium stearate since the diffraction peaks of blend shows more diffraction peaks than the pure drug Valsartan. Incompatibility observed by DSC, FTIR between Valsartan and PVP K30 was not observed by this assay.

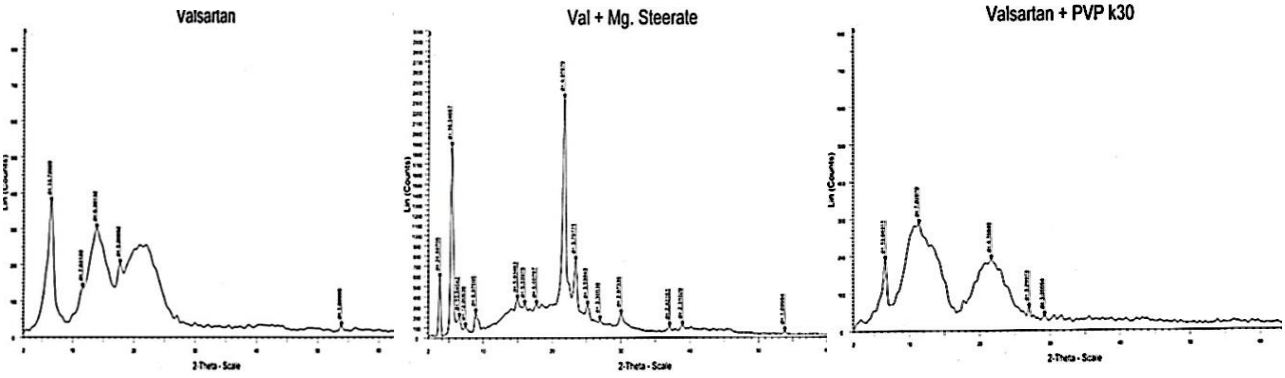

Fig.23 X–ray powder diffraction spectra of Valsartan and1:1 mass/mass blends as simple physical mixtures of Valsartan and Magnesium stearate, PVP K30.

3.2.4 Scanning electron microscopy (SEM)

SEM analysis showed the important role played in the drug–excipient physical interaction by size, shape and roughness of the excipient. In particular, in the case of PVP K30, present a characteristic popcorn-like structure and appear to be melted into large porous agglomerates, the Valsartan particles can both adhere to the surface and fill the empty spaces between agglomerates. The sample treatment (Fig.24 A), by reducing the drug crystal dimensions and by increasing the drug–excipient contact surface, favours a more complete drug dispersion in the polymeric matrix and then a greater interaction. In case of Magnesium stearate, The SEM pictures show that the characteristic flakes of the stearate are either clustered together, or attached to Valsartan crystals (Fig. 24 B) it favours more interaction and shows incompatibility.

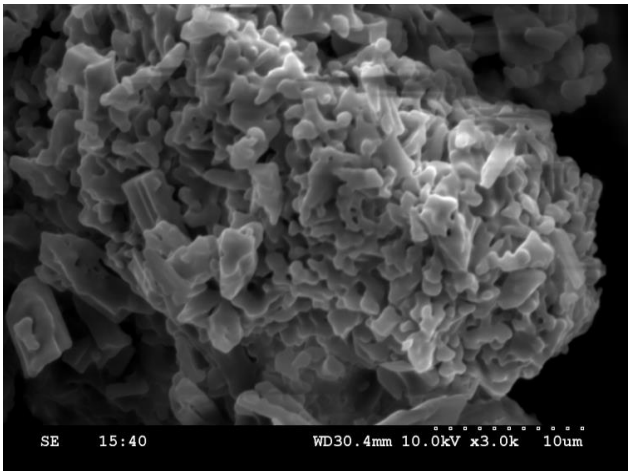

Fig.24A

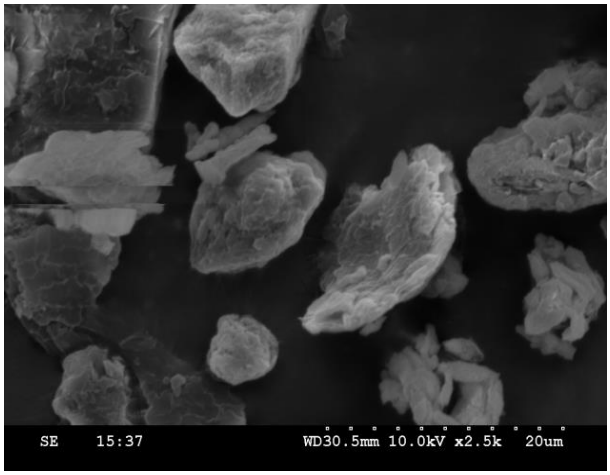

Fig.24B

Fig. 24 SEM Photomicrograph of A. Blend of Valsartan and PVP K30, B. Blend of Valsartan and Magnesium stearate

4. Conclusions

The thermal analysis provided information about the thermal stability and decomposition of pure Valsartan and the binary mixtures which can be used in the quality control. The characterization was obtained by FTIR, SEM, and XRPD, which, in turn, demonstrated Valsartan physicochemical properties including the crystallinity. In the compatibility studies, the modifications found in the DSC curves suggested a possible physical interaction of Valsartan with magnesium stearate, potato starch, PVP K30 and PEG 6000. Additional FTIR, XRPD and SEM analyses were carried out and showed strong interaction with Magnesium stearate and PVP K30 and no evidence of solid-state interaction or incompatibility with PEG 6000 and potato starch was observed.

5. Acknowledgements

The authors express their gratitude to MSN Laboratories Ltd. Hyderabad, India for providing the gift sample.

6. Conflict of Interest

No Conflict of Interest

7. Funding

No Funding

8. References:

1. Hermida RC, Calvo C, Ayala DE, Domínguez MJ, Covelo M, Fernández JR, Mojón A, López JE (2003) Administration Time–Dependent Effects of Valsartan on Ambulatory Blood Pressure in Hypertensive Subjects. Hypertension 42:283–290. https://doi.org/10.1161/01.HYP.0000084855.32823.DA
2. Potamitis C, Zervou M, Katsiaras V, Zoumpoulakis P, Durdagi S, Papadopoulos MG, Hayes JM, Grdadolnik SG, Kyrikou I, Argyropoulos D, Vatougia G, Mavromoustakos T (2009) Antihypertensive Drug Valsartan in Solution and at the AT $_1$ Receptor: Conformational Analysis, Dynamic NMR Spectroscopy, *in Silico* Docking, and Molecular Dynamics Simulations. J Chem Inf Model 49:726–739. https://doi.org/10.1021/ci800427s
3. Ushijima K, Nakashima H, Shiga T, Harada K, Ishikawa S, Ioka T, Ando H, Fujimura A (2015) Different chronotherapeutic effects of valsartan and olmesartan in non-dipper hypertensive patients during valsartan treatment at morning. Journal of Pharmacological Sciences 127:62–68. https://doi.org/10.1016/j.jphs.2014.09.004
4. Zappe DH, Palmer BF, Calhoun DA, Purkayastha D, Samuel R, Jamerson KA (2010) Effectiveness of initiating treatment with valsartan/hydrochlorothiazide in patients with stage-1 or stage-2 hypertension. J Hum Hypertens 24:483–491. https://doi.org/10.1038/jhh.2009.90
5. Lotufo PA (2005) Stroke in Brazil: a neglected disease. Sao Paulo Med J 123:3–4. https://doi.org/10.1590/S1516-31802005000100001
6. Júlio TA, Zâmara IF, Garcia JS, Trevisan MG (2013) Compatibility and stability of valsartan in a solid pharmaceutical formulation. Braz J Pharm Sci 49:645–651. https://doi.org/10.1590/S1984-82502013000400003
7. Ceschel GC, Badiello R, Ronchi C, Maffei P (2003) Degradation of components in drug formulations: a comparison between HPLC and DSC methods. Journal of Pharmaceutical and Biomedical Analysis 32:1067–1072. https://doi.org/10.1016/S0731-7085(03)00210-3
8. Desavathu M, Pathuri R, Chunduru M (2017) Design, Development and Characterization of Valsartan Microsponges by Quasi Emulsion Technique and the Impact of Stirring Rate on Microsponge Formation. J App Pharm Sci 193–198. https://doi.org/10.7324/JAPS.2017.70128
9. Çelebier M, Kaynak MS, Altınöz S, Sahin S (2010) HPLC method development for the simultaneous analysis of amlodipine and valsartan in combined dosage forms and in vitro dissolution studies. Braz J Pharm Sci 46:761–768. https://doi.org/10.1590/S1984-82502010000400018
10. Khan H (2021) Identification and characterization of degradation products of valsartan by uplc/q-tof-ms technique. Asian Journal of Pharmaceutical Research 11:1–5. https://doi.org/10.5958/2231-5691.2021.00001.0
11. Blasko A, Leahy-Dios A, Nelson WO, Austin SA, Killion RB, Visor GC, Massey IJ (2001) Revisiting the Solubility Concept of Pharmaceutical Compounds. Monatshefte fuer Chemie/Chemical Monthly 132:789–798. https://doi.org/10.1007/s007060170065
12. Liltorp K, Larsen TG, Willumsen B, Holm R (2011) Solid state compatibility studies with tablet excipients using non thermal methods. Journal of Pharmaceutical and Biomedical Analysis 55:424–428. https://doi.org/10.1016/j.jpba.2011.02.016
13. Almeida MMD, Lima CRRDC, Quenca-Guillen JS, Moscardini Filho E, Mercuri LP, Santoro MIRM, Kedor-Hackmann ERM (2010) Stability evaluation of tocopheryl acetate and ascorbyl tetraisopalmitate in isolation and incorporated in cosmetic formulations using thermal analysis. Braz J Pharm Sci 46:129–134. https://doi.org/10.1590/S1984-82502010000100015
14. Patra R, Kollati Y, Ns SK, Dirisala VR (2021) Valsartan in combination with metformin and gliclazide in diabetic rat model using developed RP-HPLC method. Futur J Pharm Sci 7:157. https://doi.org/10.1186/s43094-021-00307-2
15. Bakshi M, Singh S (2002) Development of validated stability-indicating assay methods—critical review. Journal of Pharmaceutical and Biomedical Analysis 28:1011–1040. https://doi.org/10.1016/S0731-7085(02)00047-X
16. ICH (2003) STABILITY TESTING OF NEW DRUG SUBSTANCES AND PRODUCTS Q1A(R2)

17. ICH (1996) STABILITY TESTING: PHOTOSTABILITY TESTING OF NEW DRUG SUBSTANCES AND PRODUCTS Q1B
18. ICH (2005) VALIDATION OF ANALYTICAL PROCEDURES: TEXT AND METHODOLOGY Q2(R1)
19. Divya Bhargavi P, Lolla S, Sugunan S, Shiva Gubbiyappa K, Ali Khan A, Alanazi AM, Vijay Nayak B (2023) The simultaneous quantification of Sitagliptin and Irbesartan in rat plasma using the validated LC-MS/MS method is applied to a pharmacokinetic study. Journal of Chromatography B 1221:123677. https://doi.org/10.1016/j.jchromb.2023.123677
20. Felton LA (2006) A Review of: "Pharmaceutical Stress Testing: Predicting Drug Degradation": S. W. Baertschi, ed. Taylor & Francis, Boca Raton, Fl, 2005, ISBN: 0824740211; Hardback. 482 pages. Drug Development and Industrial Pharmacy 32:505–505. https://doi.org/10.1080/03639040500529234
21. Tamizi E, Jouyban A (2016) Forced degradation studies of biopharmaceuticals: Selection of stress conditions. European Journal of Pharmaceutics and Biopharmaceutics 98:26–46. https://doi.org/10.1016/j.ejpb.2015.10.016
22. (2002) Stability of Drugs and Dosage Forms. Kluwer Academic Publishers, Boston
23. Elbaz AM, Gani A, Hourani N, Emwas A-H, Sarathy SM, Roberts WL (2015) TG/DTG, FT-ICR Mass Spectrometry, and NMR Spectroscopy Study of Heavy Fuel Oil. Energy Fuels 29:7825–7835. https://doi.org/10.1021/acs.energyfuels.5b01739